JB
Journals.ASM.org

Bacillus anthracis lcp Genes Support Vegetative Growth, Envelope Assembly, and Spore Formation

Megan Liszewski Zilla,[a,b] J. Mark Lunderberg,[a,b] Olaf Schneewind,[a,b] Dominique Missiakas[a,b]

Howard Taylor Ricketts Laboratory, Argonne National Laboratory, Lemont, Illinois, USA[a]; Department of Microbiology, University of Chicago, Chicago, Illinois, USA[b]

ABSTRACT

***Bacillus anthracis*, a spore-forming pathogen, replicates as chains of vegetative cells by regulating the separation of septal peptidoglycan. Surface (S)-layer proteins and *B. anthracis* S-layer-associated proteins (BSLs) function as chain length determinants and are assembled in the envelope by binding to the secondary cell wall polysaccharide (SCWP). *B. anthracis* expresses six different genes encoding LytR-CpsA-Psr (LCP) enzymes (*lcpB1* to *-4*, *lcpC*, and *lcpD*), which when expressed in *Staphylococcus aureus* promote attachment of wall teichoic acid to peptidoglycan. Mutations in *B. anthracis lcpB3* and *lcpD* cause aberrations in cell size and chain length that can be explained as discrete defects in SCWP assembly; however, the function of the other *lcp* genes is not known. By deleting combinations of *lcp* genes from the *B. anthracis* genome, we generated variants with single *lcp* genes. *B. anthracis* expressing *lcpB3* alone displayed physiological cell size, vegetative growth, spore formation, and S-layer assembly. Strains expressing *lcpB1* or *lcpB4* displayed defects in cell size and shape, S-layer assembly, and spore formation yet sustained vegetative growth. In contrast, the *lcpB2* strain was unable to grow unless the gene was expressed from a multicopy plasmid (*lcpB2*$^{++}$), and variants expressing *lcpC* or *lcpD* displayed severe defects in growth and cell shape. The *lcpB2*$^{++}$, *lcpC*, or *lcpD* strains supported neither S-layer assembly nor spore formation. We propose a model whereby LCP enzymes fulfill partially overlapping functions in transferring SCWP molecules to discrete sites within the bacterial envelope.**

IMPORTANCE

Products of genes essential for bacterial envelope assembly represent targets for antibiotic development. The LytR-CpsA-Psr (LCP) enzymes tether bactoprenol-linked intermediates of secondary cell wall polymers to the C6 hydroxyl of *N*-acetylmuramic acid in peptidoglycan; however, the role of LCPs as a target for antibiotic therapy is not defined. We show here that LCP enzymes are essential for the cell cycle, vegetative growth, and spore formation of *Bacillus anthracis*, the causative agent of anthrax disease. Furthermore, we assign functions for each of the six LCP enzymes, including cell size and shape, vegetative growth and sporulation, and S-layer and S-layer-associated protein assembly.

Bacillus anthracis, a Gram-positive spore-forming bacterium, infects and replicates within vertebrates, thereby precipitating anthrax disease. Without therapy, anthrax can be fatal, which triggers formation of infectious *B. anthracis* spores within the carcass (1, 2). During vegetative replication, *B. anthracis* grows as chains of rod-shaped bacteria that are tethered at septal peptidoglycan, a developmental program that protects bacteria from engulfment by phagocytes (3, 4). Earlier work identified the S-layer protein Sap, the S-layer-associated protein BslO, and the CsaB pyruvyltransferase as determinants of *B. anthracis* chain length (3, 5, 6). Both S-layer proteins (Sap and EA1) and BslO are endowed with three S-layer homology (SLH) domains, promoting association of proteins with pyruvylated secondary cell wall polysaccharide (SCWP) in the *B. anthracis* cell wall envelope (7). Mutants lacking *bslO* are defective in their ability to release cells from growing *B. anthracis* chains and thus exhibit exaggerated chain length (3). BslO, an *N*-acetylglucosaminidase, is deposited into the S-layer at the septum, where it contributes to septal peptidoglycan cleavage (3). Subcellular localization of BslO is dependent on Sap, which forms an S-layer throughout the cylindrical envelope of *B. anthracis* vegetative forms, limiting the deposition of EA1 and BslO to the cell poles in the vicinity of the septal peptidoglycan (8).

The SCWP of *B. anthracis* is composed of the repeat unit [→4)-β-ManNAc-(1→4)-β-GlcNAc-(1→6)-α-GlcNAc-(1→], where α-GlcNAc is substituted with α-Gal and β-Gal at O-3 and O-4, respectively, and β-GlcNAc is substituted with α-Gal at O-3 (9). CsaB-mediated pyruvylation of the terminal *N*-acetylmannosamine (ManNAc) is a prerequisite for SCWP binding to S-layer (Sap and EA1) and *B. anthracis* S-layer-associated proteins (BSLs) (5, 6, 10). The genetic determinants for SCWP synthesis in *B. anthracis* remain largely unknown. Nonetheless, it has been demonstrated that the ManNAc residues are supplied by GneY and GneZ, two epimerases that catalyze the stereochemical inversion at the C-2 position of UDP-GlcNAc to UDP-ManNAc (11, 12). Earlier work revealed that the SCWP is covalently attached to *B. anthracis* peptidoglycan, at least in part via murein linkage units composed of the disaccharide (GlcNAc-ManNAc) (6, 12, 13). This model is based on the observations that *tagO*, encoding undecaprenyl-phosphate *N*-acetylglucosaminyl 1-phosphate transferase, the first of two enzymes in the synthesis pathway for

Received 5 August 2015 **Accepted** 17 September 2015

Accepted manuscript posted online 21 September 2015

Citation Liszewski Zilla M, Lunderberg JM, Schneewind O, Missiakas D. 2015. *Bacillus anthracis lcp* genes support vegetative growth, envelope assembly, and spore formation. J Bacteriol 197:3731–3741. doi:10.1128/JB.00656-15.

Editor: I. B. Zhulin

Address correspondence to Dominique Missiakas, dmissiak@bsd.uchicago.edu.

Supplemental material for this article may be found at http://dx.doi.org/10.1128/JB.00656-15.

murein linkage units, is required for SCWP synthesis in *B. anthracis* (6). Furthermore, hydrofluoric acid (HF) treatment hydrolyzes phosphodiester bonds that tether SCWP to peptidoglycan (6). At least two LytR-CpsA-Psr (LCP) enzymes contribute to SCWP attachment to the *B. anthracis* peptidoglycan and the assembly of S-layers (13). *B. anthracis* encodes six LCP proteins, which have been named LcpB1 to -4, LcpC, and LcpD based on sequence comparisons with *Staphylococcus aureus* and *Bacillus subtilis* LCP enzymes (13). LCP enzymes are universal catalysts for the transfer of undecaprenyl-phosphate polymers to peptidoglycan in Gram-positive bacteria (14–17).

LCP proteins were originally identified in *B. subtilis* as TagT, TagU, and TagV and proposed to catalyze wall teichoic acid (WTA) attachment to peptidoglycan (14), specifically the formation of HF-sensitive phosphodiester bonds between the C-6 hydroxyl of *N*-acetylmuramic acid and WTA (18, 19). This activity has been shown to be shared by *S. aureus* LcpA ($LcpA_{Sa}$), $LcpB_{Sa}$, and $LcpC_{Sa}$ (16). In addition, LCP enzymes of *S. aureus* catalyze the attachment of capsular polysaccharide to peptidoglycan (17). Heterologous expression of *B. anthracis lcpB2*, *lcpB3*, *lcpB4*, *lcpC*, or *lcpD* but not *lcpB1* was shown to restore to various extents defects in staphylococcal growth and WTA attachment to peptidoglycan in *S. aureus* variants lacking all three *lcp* genes (Δ*lcpABC*) (13). Loss of *lcpB3* or *lcpD* in *B. anthracis* produced cells with altered size and chain-length phenotypes that can be explained by defects in S-layer and SCWP assembly (13). Together these observations suggest that LCP enzymes recognize undecaprenolpyrophosphate-linked amino sugars as the substrates for transfer to peptidoglycan.

The phenotypic analyses of mutants lacking individual *lcp* genes could not explain why *B. anthracis* evolved six LCP enzymes when *B. subtilis* and *S. aureus* elaborate only three. Unlike *B. subtilis* or *S. aureus*, *B. anthracis* does not synthesize WTA or capsular polysaccharide. Here, we developed *B. anthracis* variants expressing only one of the six genes for LCP enzymes. Based on the phenotypic analyses of these variants, we propose a model to account for the expanded repertoire of *B. anthracis* LCP enzymes and their contribution to SCWP attachment to peptidoglycan.

MATERIALS AND METHODS

Bacterial growth and reagents. *B. anthracis* strain Sterne 34F2 (20) and its variants were grown in brain heart infusion (BHI) broth or agar at 37°C. *Escherichia coli* K1077 (21) was grown in Luria-Bertani (LB) broth or agar at 37°C. Where necessary, ampicillin (Amp [100 μg/ml]), chloramphenicol (Cm [10 μg/ml]), spectinomycin (Sp [200 μg/ml]), or kanamycin (Kan [20 μg/ml]) was added to cultures. *B. anthracis* strains were sporulated in modified G medium (modG) (22). Spore preparations were heat treated at 68°C for 30 min to kill vegetative bacilli. Spore titers were determined by plating aliquots of serially diluted spore preparations on LB agar; CFU were enumerated after overnight incubation at 30°C. To examine growth, overnight cultures were normalized to an absorbance at 600 nm (A_{600}) of 5 and diluted 1:100 into 100 μl fresh BHI medium, and growth at 37°C was monitored every 30 min for 12 h in a Synergy HT plate reader (BioTek) by recording the A_{600}. For measurements of growth rate, *r*, the exponential growth phase for each resulting growth curve was fit to the equation $A^t = A^0 \times e^{rt}$, where A^t is absorbance at time *t*, A^0 is the initial absorbance, and *t* is the time elapsed between A^0 and A^t recordings. To assess viability, aliquots were removed at 6 h, serially diluted, plated on LB agar, and grown overnight at 30°C.

Bacterial strains and plasmids. The bacterial strains and plasmids utilized in this study are listed in Table 1. *B. anthracis* Sterne($pXO1^+$, $pXO2^-$) was used as the parent wild-type (WT) strain. The alleles *lcpB2*::*kan* and *lcpD*::*spec* were obtained by transposon mutagenesis with *bursa aurealis* (23) and have been described earlier (13). Deletion of *lcpB1*, *lcpB3*, *lcpB4*, or *lcpC* was achieved by allelic replacement using the temperature-sensitive vector pLM4 (13, 24, 25). The process was repeated as needed to replace genes with unmarked alleles in a single background. For marked alleles such as *lcpB2*::*kan* and *lcpD*::*spec*, bacteriophage CP51 was used to transduce the resistance traits into wild-type *B. anthracis* Sterne and isogenic *lcp* allelic variants (26). Transductants were verified by DNA sequencing of inverse PCR products as previously described (23). Unmarked mutant alleles were verified by PCR using primers flanking the cloning sites. The sequences of the primers used for this study were described previously (13).

Microscopy. The chain lengths of bacilli were determined by analyzing microscopy images (3). Briefly, *B. anthracis* cultures were normalized by measuring an A_{600} of 5 and diluted 1:100 into BHI broth at 37°C. At defined time points, aliquots of cells were removed and then fixed with 4% formalin, and images were captured with a charge-coupled device (CCD) camera on an Olympus IX81 microscope using 20× or 40× objectives. Chain lengths of bacilli were measured from acquired differential interference contrast (DIC) images using ImageJ and converted to lengths in micrometers using reference images of an objective micrometer (3). Cell lengths were assessed in the same manner, except that cell septa were stained with boron dipyrromethene vancomycin (B-vancomycin [Invitrogen]), and images were obtained with a 100× objective. The statistical significance of length distributions between different strains was analyzed using a one-way analysis of variance (ANOVA).

For fluorescence microscopy, *B. anthracis* cultures were normalized to an A_{600} of 5, diluted 1:100 into BHI, and incubated for either 2 or 8 h at 37°C before cells were fixed with 4% formalin. After extensive rinsing, samples were incubated with rabbit antisera raised against purified Sap, EA1, or BslO, and bound antibodies were detected with DyLight594-conjugated anti-rabbit IgG secondary antibody. Cells were counterstained with B-vancomycin. A Leica SP5 STED-CW superresolution laser scanning confocal microscope with a 63× objective was used to analyze the fluorescence of *B. anthracis* cells as described previously (27).

S-layer fractionation. *B. anthracis* cultures normalized to an A_{600} of 5 were diluted 1:100 into BHI broth and grown at 37°C until cultures reached an A_{600} of 2. One milliliter of culture was sedimented by centrifugation, and the supernatant (medium fraction) was transferred to a new tube. Cells in the sediment were washed with phosphate-buffered saline (PBS) twice, sedimented, and suspended in PBS buffer containing 3 M urea. The samples were heated at 95°C for 10 min and centrifuged (10,000 × *g*, 10 min), and the supernatants containing S-layer and S-layer-associated proteins (S-layer fraction) were transferred to a new tube. The bacterial sediment was washed with PBS and mechanically lysed by silica bead beating. After sedimentation of the beads (1,000 ×*g*, 1 min), the lysate (cellular fraction) was transferred to a third tube. Proteins in the medium, S-layer, and cellular fractions were precipitated by addition of trichloroacetic acid (TCA [10% final concentration]). Precipitates were collected by centrifugation (10,000 × *g*, 10 min), washed with acetone, air dried, suspended in 100 μl of 1 M Tris-HCl (pH 8.0)–4% SDS, and mixed with an equal volume of SDS-PAGE loading buffer. Proteins in samples were separated by SDS-PAGE and visualized by Coomassie staining or transferred to polyvinylidene difluoride membrane for immunoblot analysis using rabbit antisera raised against purified antigens. Immunoreactive products were revealed by chemiluminescent detection after incubation with horseradish peroxidase (HRP)-conjugated secondary antibody (Cell Signaling Technology).

RESULTS

LytR-CpsA-Psr proteins are required for *B. anthracis* growth. To analyze the function of different LCP enzymes in *B. anthracis*, we chose to generate six strains that each express a single *lcp* gene. The coding sequences of four genes—*lcpB1* (BAS1830), *lcpB3* (BAS0746), *lcpB4* (BAS3381), and *lcpC* (BAS5115)—were deleted

TABLE 1 *B. anthracis* strains used in this study

Strain genotype	Designation	Description[a]	Reference or source
WT	Sterne 34F2	WT (pXO1$^+$, pXO2$^-$)	20
Variants			
lcpB2::*aphA3* Δ*lcpB3B4C lcpD*::*aad9*	*lcpB1*$^+$ strain	*lcpB3* (BAS0746) (deletion, nt 798568–799746), *lcpB4* (BAS3381) (deletion, nt 3356447–3357475), *lcpC* (BAS5115) (deletion, nt 4995461–4994610), *lcpB2* (BAS0572)::*aphA3* (insertion, nt 619533), *lcpD* (BAS5047)::*aad9* (insertion, nt 4919831)	This work
Δ*lcpB1B3B4C lcpD*::*aad9*/p*lcpB2*	*lcpB2*$^{++}$ strain	*lcpB1* (BAS1830) (deletion, nt 1856993–1857982), *lcpB3* (BAS0746) (deletion, nt 798568–799746), *lcpB4* (BAS3381) (deletion, nt 3356447–3357475), *lcpC* (BAS5115) (deletion, nt 4995461–4994610), *lcpD* (BAS5047)::*aad9* (insertion, nt 4919831); p*lcpB2* is pWWW412 with *lcpB2* (BAS0572)	This work
Δ*lcpB1 lcpB2*::*aphA3* Δ*lcpB4C lcpD*::*aad9*	*lcpB3*$^+$ strain	*lcpB1* (BAS1830) (deletion, nt 1856993–1857982), *lcpB4* (BAS3381) (deletion, nt 3356447–3357475), *lcpC* (BAS5115) (deletion, nt 4995461–4994610), *lcpB2* (BAS0572)::*aphA3* (insertion, nt 619533), *lcpD* (BAS5047)::*aad9* (insertion, nt 4919831)	This work
Δ*lcpB1 lcpB2*::*aphA3* Δ*lcpB3C lcpD*::*aad9*	*lcpB4*$^+$ strain	*lcpB1* (BAS1830) (deletion, nt 1856993–1857982), *lcpB3* (BAS0746) (deletion, nt 798568–799746), *lcpC* (BAS5115) (deletion, nt 4995461–4994610), *lcpB2* (BAS0572)::*aphA3* (insertion, nt 619533), *lcpD* (BAS5047)::*aad9* (insertion, nt 4919831)	This work
Δ*lcpB1 lcpB2*::*aphA3* Δ*lcpB3B4 lcpD*::*aad9*	*lcpC*$^+$ strain	*lcpB1* (BAS1830) (deletion, nt 1856993–1857982), *lcpB3* (BAS0746) (deletion, nt 798568–799746), *lcpB4* (BAS3381) (deletion, nt 3356447–3357475), *lcpB2* (BAS0572)::*aphA3* (insertion, nt 619533), *lcpD* (BAS5047)::*aad9* (insertion, nt 4919831)	This work
Δ*lcpB1 lcpB2*::*aphA3* Δ*lcpB3B4C*	*lcpD*$^+$ strain	*lcpB1* (BAS1830) (deletion, nt 1856993–1857982), *lcpB3* (BAS0746) (deletion, nt 798568–799746), *lcpB4* (BAS3381) (deletion, nt 3356447–3357475), *lcpC* (BAS5115) (deletion, nt 4995461–4994610), *lcpB2* (BAS0572)::*aphA3* (insertion, nt 619533)	This work
Δ*sap*	*sap* strain	*sap* (BAS0841) (deletion, nt 896758–899063)	27
Δ*eag*	*eag* strain	*eag* (BAS0842) (deletion, nt 899843–902414)	27
bslO::*aad9*	*bslO* strain	*bslO* (BAS1683)::*aad9* (insertion, nt 1703151)	3

[a] The nucleotide numbers provided in this column correspond to nucleotide positions in the sequenced genome of the Sterne strain as described in the NCBI databank under accession no. NC_005945.

from the chromosome of *B. anthracis* Sterne 34F2 by allelic replacement either alone or as combinations with two, three, or four deletions. Bacteriophage CP51 was used to generate lysates of *B. anthracis lcpB2*::*kan* (*lcpB2* = BAS0572) and *lcpD*::*spec* (*lcpD* = BAS5047) strains isolated following mutagenesis with the *bursa aurealis* minitransposon carrying kanamycin (*aphA3*) and spectinomycin (*aad9*) resistance markers, respectively. *lcpB2*::*aphA3* and/or *lcpD*::*aad9* was then transduced into *B. anthracis* mutants with deletions in three or four *lcp* genes. As a result, five new strains of the genotypes *lcpB1*$^+$, *lcpB3*$^+$, *lcpB4*$^+$, *lcpC*$^+$, and *lcpD*$^+$ were generated (Table 1). Each strain was designated after the only remaining *lcp* gene. For example, the *lcpB1*$^+$ strain carries *lcpB1* on the chromosome but no longer carries *lcpB2*, *lcpB3*, *lcpB4*, *lcpC*, and *lcpD*. We were unable to transduce *lcpD*::*aad9* into the Δ*lcpB1* Δ*lcpB3* Δ*lcpB4* Δ*lcpC* background unless the variant had been transformed with p*lcpB2*, a high-copy-number plasmid for *lcpB2* overexpression (Fig. 1A; Table 1). As a control, the *B. anthracis* Δ*lcpB1* Δ*lcpB3* Δ*lcpB4* Δ*lcpC* strain transformed with the control vector (pWWW412) could not be transduced with CP51 lysate from the *B. anthracis lcpD*::*aad9* strain (Fig. 1A). The sixth variant is thus a merodiploid strain that carries two copies of the *lcpB2* gene and thus is designated by the genotype *lcpB2*$^{++}$ (Table 1). Together, these data indicate that expression of chromosomal *lcpB1*$^+$, *lcpB3*$^+$, *lcpB4*$^+$, *lcpC*$^+$ or *lcpD*$^+$ alone was sufficient to support *B. anthracis* vegetative growth, whereas expression of *lcpB2*$^+$ was not. Nevertheless, when *lcpB2* was overexpressed from a plasmid, *lcpB2*$^{++}$ supported *B. anthracis* vegetative growth in the absence of the other five *lcp* genes. The data suggest further that expression of *lcp* genes is essential for *B. anthracis* vegetative growth.

To quantify vegetative growth, overnight cultures of *B. anthracis* were normalized for A_{600}, diluted 100× into fresh medium, and incubated with rotation at 37°C while monitoring vegetative expansion as increases in A_{600} (Fig. 1B). These growth curves were used to deduce growth rates of 0.488, 0.498, 0.542, 0.496, 0.471, 0.350, and 0.253 h^{-1}, respectively, for the wild-type and *lcpB1*$^+$, *lcpB2*$^{++}$, *lcpB3*$^+$, *lcpB4*$^+$, *lcpC*$^+$, and *lcpD*$^+$ strains. An aliquot of cultures was removed at 6 h, diluted serially, and spotted on agar plates for enumeration of colonies (Fig. 1C). The *lcpB3*$^+$ variant grew at the same rate as the wild type and displayed similar plating efficiency (Fig. 1B and C). In contrast, the *lcpD*$^+$ variant displayed a severe growth defect, with an extended lag phase (Fig. 1B) and

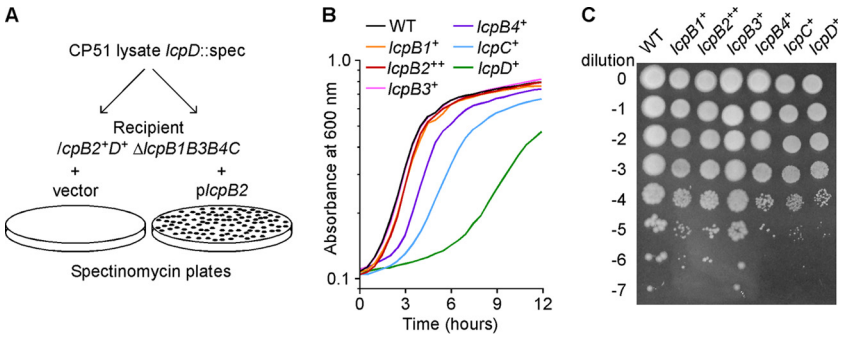

FIG 1 Growth and viability of *B. anthracis* variants expressing single *lcp* genes. (A) The Δ*lcpB1B3B4C* quadruple mutant, which still carries the *lcpB2* and *lcpD* genes, was transformed with a plasmid containing *lcpB2* (p*lcpB2*) or the cloning vector, and these strains were used as recipient strains for transduction of the *lcpD*::*aad9* allele using bacteriophage CP51. The p*lcpB2*-bearing strain is merodiploid for *lcpB2*. Following transduction, bacteria were plated on spectinomycin-containing medium and incubated at 30°C for 30 h. Recombination of the *lcpD*::*aad9* allele was verified by DNA sequencing and occurred only in the merodiploid strain. (B) Overnight cultures of wild-type (WT) *B. anthracis* Sterne and isogenic variants expressing a single *lcp* gene were normalized to A_{600} of 5, diluted 1:100 into fresh medium, and grown at 37°C. Growth was monitored by recording the change in cell density (absorbance) at 600 nm every 30 min over 12 h. (C) After 6 h following dilution in fresh medium (as described for panel B), cultures were serially diluted, and 5-μl aliquots of each serial 10-fold dilution (0 through −7) were plated on agar medium. An image of the plate after overnight incubation at 30°C is shown.

diminished vegetative expansion (Fig. 1C). The *lcpC*$^+$ and *lcpB4*$^+$ variants grew more slowly than the wild type but expanded faster than the *lcpD*$^+$ mutant. Of note, the 6-h plating efficiency of the *lcpC*$^+$ and *lcpB4*$^+$ strains was reduced to the same level as the *lcpD*$^+$ mutant, suggesting that not all vegetative expansion of *lcpC*$^+$ and *lcpB4*$^+$ generates viable cells. Finally, the *lcpB1*$^+$ and *lcpB2*$^{++}$ variants displayed slight reductions in vegetative expansion and plating efficiency compared to the *B. anthracis* wild type or the *lcpB3*$^+$ variant. These data indicate that, in the absence of the other LCP enzymes, only LcpB3 is sufficient to support *B. anthracis* vegetative growth at wild-type levels.

Cell size and chain length of *lcp* variant *B. anthracis*. *B. anthracis* varies the chain length of vegetative cells by regulating the separation of septal peptidoglycan. As reported before, chain lengths of wild-type bacilli were increased 2 h following dilution of overnight cultures into fresh medium and were subsequently reduced in a stepwise fashion, as vegetative bacilli approached stationary phase. Earlier work showed that the *B. anthracis lcpD* mutant displayed an increased chain length, whereas the *lcpB3* variant formed shorter chains with cells that are smaller than their wild-type counterparts (13). Overnight cultures of *B. anthracis* variants were diluted 100-fold, and fixed aliquots, withdrawn at hourly intervals, were analyzed by DIC microscopy for chain length (Fig. 2A; see Fig. S1 in the supplemental material). The average chain length of the *lcpB1*$^+$, *lcpB4*$^+$, *lcpC*$^+$, and *lcpD*$^+$ variants was diminished at 2 h, whereas the *lcpB2*$^{++}$, *lcpB3*$^+$, *lcpB4*$^+$, and *lcpD*$^+$ strains displayed increased chain lengths at one or more time points (marked with asterisks in Fig. 2A). The average chain length of the *lcpB4*$^+$ variant was particularly exaggerated; at the 4-h time interval, the median chain length of *lcpB4*$^+$ bacilli was 73 μm, compared to a median of 11 μm for wild-type *B. anthracis*. Thus, none of the six LCP enzymes alone is sufficient to impose physiological control of *B. anthracis* chain length, which appears to require multiple LCP proteins, if not a full complement of these enzymes.

Microscopy experiments revealed also aberrant cell shapes of the *lcp* variants. To quantify these differences, the length of 150 individual cells was measured at the 4- and 8-h time intervals after specimens were stained with BODIPY-vancomycin to visualize peptidoglycan and cell septa (Fig. 2B). The *lcpB4*$^+$ variant displayed the greatest variation in cell shape and size from wild-type bacilli. At 4 h, the *lcpB4*$^+$ strain placed septal peptidoglycan in irregular intervals, generating cells that were either very short, of extended length, or with a widened, deformed shape (Fig. 2B). By 8 h, the *lcpB4*$^+$ strain formed cells that were significantly longer than wild-type bacilli; indeed some cells reached a length of 10 μm and did not form septal peptidoglycan (Fig. 2B). Cells from the *lcpB1*$^+$, *lcpC*$^+$, and *lcpD*$^+$ strains were significantly shorter than wild-type bacilli at both 4 and 8 h postinoculation (Fig. 2B). Shortened cell size was associated with cell rounding, and the *lcpB1*$^+$, *lcpC*$^+$, and *lcpD*$^+$ mutants appeared to form chains of cocci (Fig. 2B). *lcpB2*$^{++}$ cells were only slightly elongated at 4 h but otherwise retained the morphological features of wild-type *B. anthracis*. Finally, the *lcpB3*$^+$ strain formed cells with a physiological size that could not be distinguished from wild-type bacilli.

***lcpC*$^+$ and *lcpD*$^+$ variants cannot assemble *B. anthracis* S-layers.** The ability of single *lcp* variants to assemble an S-layer was analyzed by fractionating *B. anthracis* cultures. Cultures were centrifuged, and the extracellular medium (M) was separated from the bacterial sediment. The S-layer (S) was solubilized by extraction with 3 M urea, which, following sample centrifugation, was separated with the supernatant from bacterial cells. Murein sacculi of *B. anthracis* were disrupted by bead beating to generate a cell lysate (C). Proteins in all fractions were precipitated with TCA, separated by SDS-PAGE, and analyzed by Coomassie blue staining (Fig. 3A). In wild-type *B. anthracis*, S-layer proteins Sap and EA1 are the most abundant polypeptides in fractionated cultures in the S-layer and medium fractions of Coomassie-stained SDS-PAGE (Fig. 3A, arrow). The *lcpC*$^+$ and *lcpD*$^+$ strains did not assemble detectable S-layers, whereas the *lcpB2*$^{++}$ strain assembled dramatically reduced amounts of Sap and EA1 in the envelope, and the *lcpB4*$^+$ strain assembled a diminished EA1 S-layer (Fig. 3A). The *lcpB1*$^+$ and *lcpB3*$^+$ strains assembled S-layer proteins in the bacterial envelope in a manner similar to that of wild-type *B. anthracis* (Fig. 3A).

Immunoblotting experiments revealed that the *lcpC*$^+$ and *lcpD*$^+$ strains assembled small amounts of Sap and EA1 in the bacterial envelope (Fig. 3B). Immunoblotting experiments other-

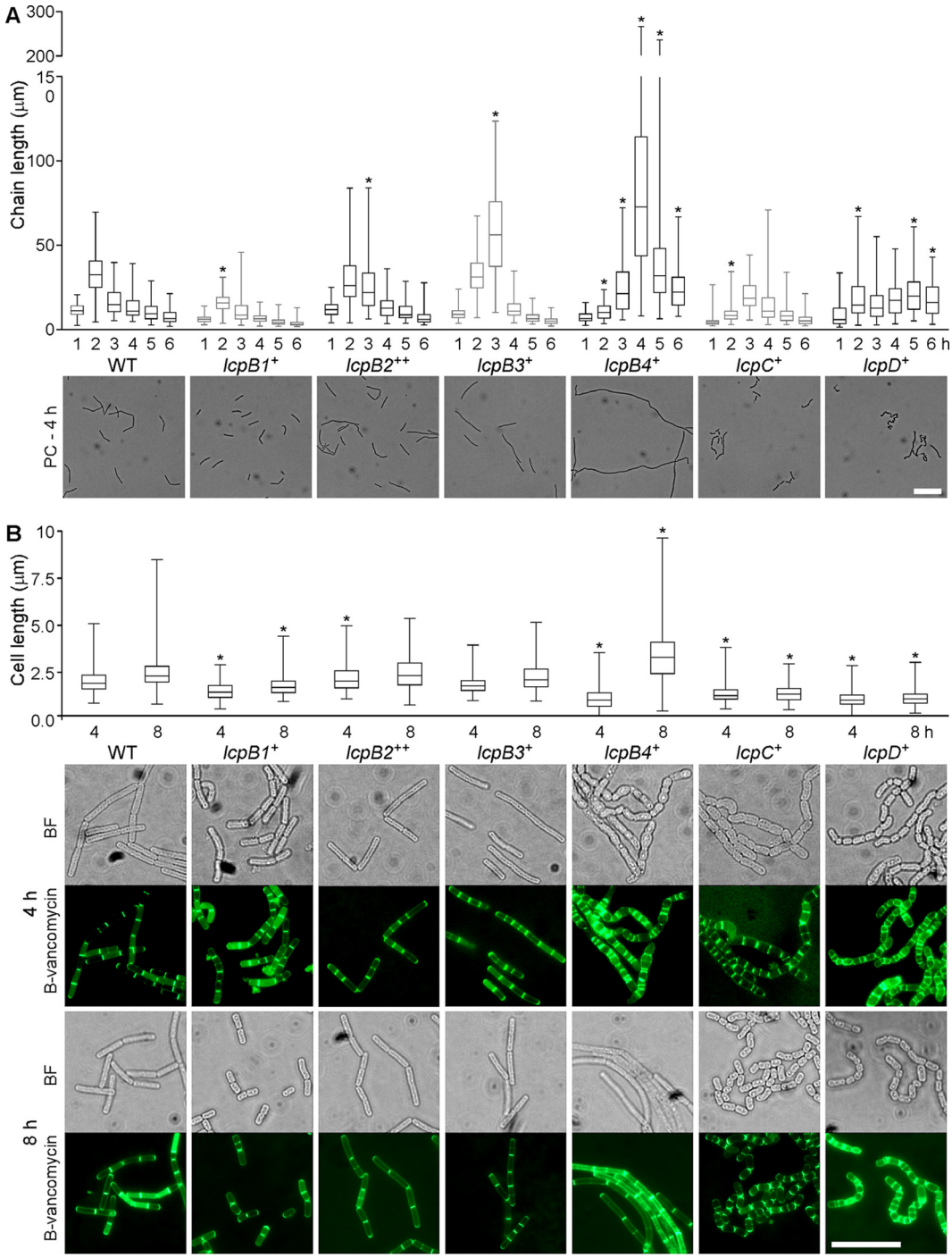

FIG 2 Chain length and cell length of *B. anthracis* variants expressing single *lcp* genes. (A) Aliquots of cultures grown as described for Fig. 1B were removed and fixed at hourly intervals for up to 6 h following inoculation in fresh medium. Images were captured and used to measure the lengths of 100 chains per time point using the ImageJ software. Results are presented in a box-and-whisker plot, where the box denotes the 25th and 75th percentiles, the whiskers denote the minimum and maximum values, and the center bar indicates the median value. Representative phase-contrast (PC) microscopy images from the 4-h time point are shown beneath the plot. The scale bar represents 20 μm. (B) Aliquots of cultures fixed at 4 and 8 h following inoculation in fresh medium were stained with BODIPY-vancomycin (B-vancomycin). The lengths of individual cells ($n > 150$) were measured using the ImageJ software and are presented in a box-and-whisker plot as in panel A. Representative images from both time points are shown below the plot, with bright-field (BF) microscopy images on top and images of the specimen stained with B-vancomycin below. The scale bar represents 10 μm. Data were analyzed by ANOVA for significant differences compared to the WT at the same time point. *, $P < 0.05$.

wise confirmed Coomassie-stained SDS-PAGE data on S-layer protein assembly. We also used immunoblotting to analyze the assembly of S-layer-associated proteins in the envelope of *B. anthracis* strains (Fig. 3B). The assembly of the murein hydrolases BslO, BslS, BslT, and BslU was diminished in the *lcpD*$^+$ strain yet unaffected in the *lcpC*$^+$ strain or in any of the other single-*lcp*-gene-expressing strains. Immunoblotting with anti-BslR revealed the reciprocal phenotype with increased envelope assembly of the

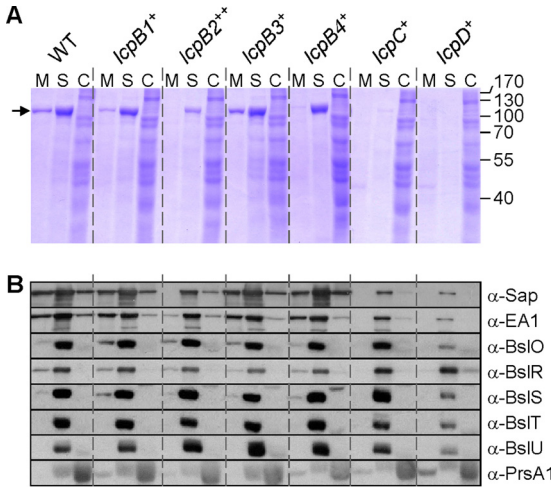

FIG 3 Subcellular fractionation of proteins with SLH domains. (A) Cultures of wild-type (WT) *B. anthracis*, carrying all six *lcp* genes or of variants with a single *lcp* gene (*lcpB1*$^+$, *lcpB2*$^{++}$, *lcpB3*$^+$, *lcpB4*$^+$, *lcpC*$^+$, or *lcpD*$^+$) were grown to an A_{600} of 2. Cultures were centrifuged to separate the extracellular medium (M) from the bacterial sediment. Proteins in the S layers (S) were extracted by boiling cells in 3 M urea. Stripped cells were broken mechanically to release cytosolic extracts (C). Proteins in all fractions were precipitated with TCA, washed in acetone, and separated by 10% SDS-PAGE. The gel was stained with Coomassie brilliant blue. The positions of Sap and EA1 that migrate with the same mobility on SDS-PAGE and of molecular mass markers are indicated by an arrow, and masses are given in kilodaltons on the right. (B) *B. anthracis* cultures fractionated as described for panel A were subjected to immunoblotting with rabbit antisera raised against purified Sap, EA1, BslO, BslR, BslS, BslT, BslU, or PrsA1.

BslR murein hydrolase in *lcpC*$^+$ and *lcpD*$^+$ strains compared to wild-type and *lcpB1*$^+$, *lcpB2*$^{++}$, *lcpB3*$^+$, or *lcpB4*$^+$ strains (Fig. 3B). As a control, immunoblotting experiments suggested that the abundance and subcellular distribution of PrsA, a secreted lipoprotein, were similar between wild-type and *lcp* variant strains. Together, these data showed that the capacity for S-layer assembly is greater in *B. anthracis* variants expressing single LcpB-type enzymes (*lcpB1*$^+$, *lcpB2*$^{++}$, *lcpB3*$^+$, or *lcpB4*$^+$) than in strains producing LcpC or LcpD.

The *lcpB3*$^+$ variant generates a physiological distribution of S-layer and S-layer-associated proteins. Next, microscopy was used to visualize the deposition and localization of S-layer and S-layer-associated proteins on the surface of bacilli. Overnight cultures of *B. anthracis* were diluted into fresh medium and incubated with rotation, and aliquots were withdrawn at timed intervals. Cells were fixed and incubated with rabbit immune sera raised against purified Sap, EA1, or BslO, as well as secondary antibody conjugated to fluorophore (Fig. 4 and 5). B-vancomycin staining was used to reveal cell septa. As expected, wild-type *B. anthracis* assembled homogeneous Sap S-layers along the cylindrical envelope of bacteria, whereas EA1 S-layers as well as BslO were deposited in the vicinity of septal peptidoglycan (Fig. 4 and 5). The *lcpD*$^+$ strain assembled neither cylindrical S-layers with Sap nor EA1 S-layers in the vicinity of septal peptidoglycan; instead, *lcpD*$^+$ cells revealed punctate EA1 deposits, irregular Sap assemblies (Fig. 4), and a cylindrical deposition of BslO (Fig. 5). The *lcpC*$^+$ variant generated cylindrical Sap assemblies and punctate EA1 deposits that colocalized with B-vancomycin staining of shortened bacilli (Fig. 4). Nevertheless, the *lcpC*$^+$ variant mislocalized BslO, which was found throughout the cylindrical envelope (Fig. 5). A similar phenotype was revealed for the *lcpB1*$^+$ variant, albeit the overall amount of EA1 staining in *lcpB1*$^+$ cells was higher than that of *lcpC*$^+$ bacilli (Fig. 4). The *lcpB2*$^+$ and *lcpB4*$^+$ variants mislocalized EA1 and BslO, which were detected in large patches throughout the cylindrical envelope; this phenotype was associated with areas of diminished Sap S-layer assembly (Fig. 4 and 5). Of note, the *lcpB4*$^+$ variant formed aberrant cells with increased diameter and irregular shape, which were generally devoid of Sap or EA1 assemblies. Only the *lcpB3*$^+$ variant assembled cylindrical Sap and septal EA1 S-layers with septal BslO deposits in a manner similar to wild-type *B. anthracis* (Fig. 4 and 5).

Only *lcpB3*$^+$ is fully sufficient for *B. anthracis* spore formation. During sporulation, *B. anthracis* directs septum formation in the vicinity of one of the two cell poles, thereby generating large mother cells and smaller forespores, which are then developed further into heat-resistant spores. We wondered whether LCP enzymes are required for this process. Overnight cultures of wild-type *B. anthracis* and its *lcp*$^+$ variants were washed and suspended in modG medium at an A_{600} of 1 to initiate sporulation. At timed intervals, culture aliquots were withdrawn, heat treated (68°C to kill vegetative bacilli), serially diluted, and spread on agar plates to enumerate CFU of heat-resistant spores. At time zero, *B. anthracis* cultures in modG medium harbored similar amounts of vegetative bacilli without spores (Fig. 6A). After 24 h of incubation in modG medium, spore formation in wild-type *B. anthracis* had been completed, and further incubation for 48 or 96 h did not result in elevated spore counts (Fig. 6B). The *lcpB3*$^+$ variant sporulated with similar efficiency to wild-type *B. anthracis*, whereas the *lcpB2*$^{++}$, *lcpC*$^+$, and *lcpD*$^+$ strains failed to produce spores (Fig. 6A and B). The *lcpB1*$^+$ and *lcpB4*$^+$ strains generated spores, albeit with 1,000- to 10,000-fold reduced efficacy (Fig. 6A and B). Microscopic examination of *B. anthracis* incubated in modG medium confirmed these observations. Refractile spores were readily visualized in samples from wild-type and *lcpB3*$^+$ *B. anthracis*, whereas spores could rarely be detected in samples of the *lcpB1*$^+$ and *lcpB4*$^+$ variants (Fig. 6C).

Aliquots of sporulating *B. anthracis* that had been removed 3 and 8 h following suspension in modG medium at an A_{600} of 5 were stained with FM4-64 and B-vancomycin for visualization of membranes and septal peptidoglycan (see Fig. S2 in the supplemental material). In the wild-type and *lcpB3*$^+$ strains of *B. anthracis*, these experiments revealed asymmetric cell division sites and forespore engulfment after 3 h of incubation as well as spore formation after 8 h. Asymmetric cell division and forespore engulfment were not detected in the *lcpB2*$^{++}$, *lcpC*$^+$, and *lcpD*$^+$ strains, suggesting that these variants did not initiate the early stages of spore formation.

DISCUSSION

B. subtilis, a spore-forming Gram-positive microbe, has been studied in depth as a model organism for bacterial development, cell biology, and industrial production of enzymes. Earlier work characterized the chemical structure of peptidoglycan and attached secondary cell wall polymers, including polyglycerol-phosphate wall teichoic acid (WTA), minor polyribitol-phosphate teichoic acid (TA), and teichuronic acid (TU) (reviewed in reference 28). Other studies identified genetic determinants for the synthesis of WTA, TA, and TU, which are located within a 50-kb region on the *B. subtilis* genome (reviewed in reference 29). *B.*

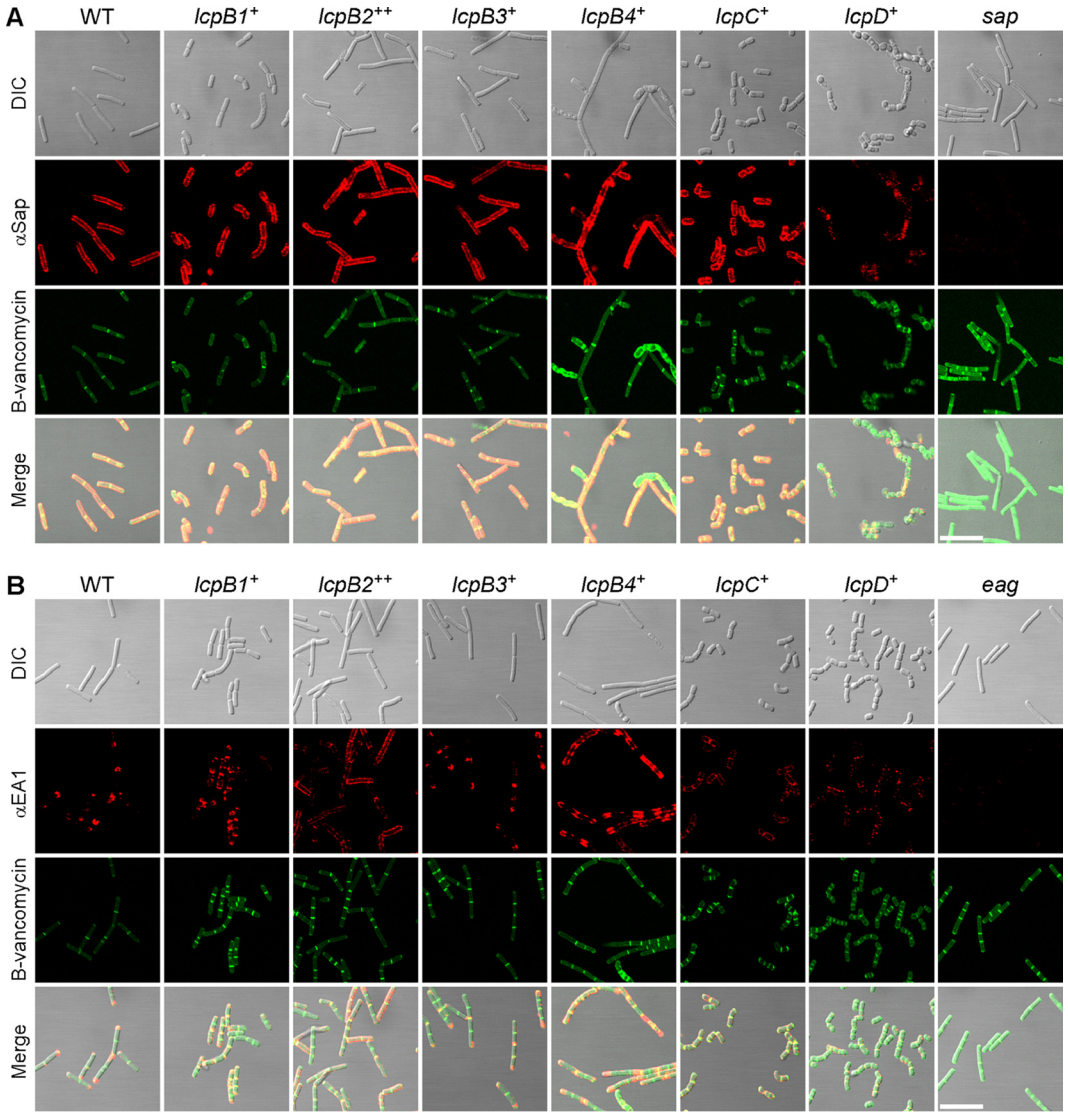

FIG 4 Deposition of S-layer proteins in the envelope of *lcp* variants. *B. anthracis* Sterne (WT) and isogenic variants carrying a single *lcp* gene were fixed in 4% buffered formalin at 8 h following inoculation of cultures in fresh medium. The localization of Sap (A) and EA1 (B) was observed with specific rabbit antisera as well as secondary antibody conjugates and counterstained with B-vancomycin to reveal the septal peptidoglycan. As controls, *sap* and *eag* mutants were also stained with their respective antisera. DIC, fluorescence, and merged microscopy images are shown for each strain. Scale bars represent 10 μm.

subtilis employs three genes for LCP enzymes to assemble secondary wall polymers in the bacterial envelope. The genetic determinants—*tagT*, *tagU*, and *tagV*—are located in the 50-kb region for secondary cell wall polymer synthesis (14). *B. subtilis* strains lacking all three genes (Δ*tagTUV*) cannot grow; however, this growth phenotype is suppressed by mutations in *tagO* (14). As TagO catalyzes the first step in the synthesis pathway for murein linkage units (30), *B. subtilis tagO* strains suppress the growth phenotype of Δ*tagTUV* mutants via feedback inhibition of undecaprenol-phosphate-linked intermediates in the synthesis pathway for secondary cell wall polymers. *B. subtilis* mutants lacking combinations of two genes for LCP enzymes do not display significant phenotypes (14). These data suggest that LCP enzymes of *B. subtilis* display overlapping and redundant functions in tethering murein linkage units with appended WTA, TA, or TU to the bacterial peptidoglycan.

S. aureus, a Gram-positive pathogen that does not form spores, attaches polyribitol-phosphate wall teichoic acid (WTA) and capsular polysaccharide to the peptidoglycan envelope (16, 17, 31). Three LCP enzymes—encoded by *lcpA*, *lcpB*, and *lcpC*—fulfill overlapping and partially redundant functions, anchoring murein linkage units with appended WTA or capsular polysaccharide to peptidoglycan. Functional redundancy has also been observed for LCP-mediated attachment of capsular polysaccharide in *Streptococcus pneumoniae* (15). In *S. aureus*, deletion of *lcpC* primarily affects cell wall attachment of the capsular polysaccharide (16), whereas deletion of *lcpA* and *lcpB* imposes defects in *S. aureus* WTA synthesis (17). Similar to *B. subtilis*, *S. aureus* mutants with defects in WTA synthesis machinery downstream of the TagO/TagA-derived murein linkage unit cannot replicate, and this phenotype is suppressed by mutations in *tagO* (32, 33). Nevertheless, *S. aureus* mutants lacking all three genes for LCP enzymes

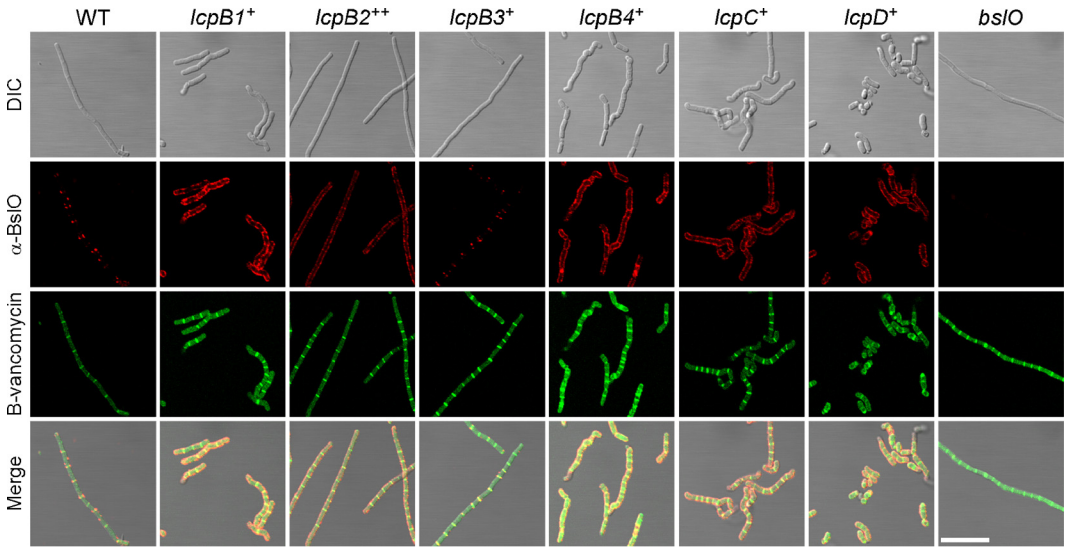

FIG 5 Deposition of S-layer-associated proteins in the envelope of *lcp* variants. *B. anthracis* Sterne (WT) and isogenic variants carrying a single *lcp* gene were fixed in 4% buffered formalin at 2 h following inoculation of cultures in fresh medium. The localization of BslO was observed with specific rabbit antisera as well as secondary antibody conjugates and counterstained with B-vancomycin to reveal the septal peptidoglycan. As a control, *bslO* mutant bacilli were also stained with their respective antisera. DIC, fluorescence, and merged microscopy images are shown for each strain. Scale bars represent 10 μm.

(Δ*lcpABC*) are capable of growth, albeit at a reduced rate (16, 31). The reduced growth phenotype of *S. aureus* Δ*lcpABC* mutants is not suppressed by *tagO* mutations (16). Expression of *B. anthracis lcpB2*, *lcpB3*, *lcpB4*, *lcpC*, or *lcpD* but not of *lcpB1* can restore some of the defects in staphylococcal growth and WTA assembly in *S. aureus* Δ*lcpABC* mutants (13). These data suggest that LCP enzymes of *S. aureus* and *B. anthracis* have evolved substrate preferences, recognizing murein linkage units with attached carbohydrate polymers or undecaprenol-phosphate-linked polysaccharides without murein linkage units.

B. anthracis does not synthesize WTA (34), and a thorough search of its genome does not identify homologs of the *B. subtilis* genes for TU synthesis. Unlike *S. aureus* and *B. subtilis*, *B. anthracis* attaches SCWP in the bacterial cell wall envelope and uses its CsaB-pyruvylated and PatA1/PatB1- or PatA2/PatB2-acetylated derivatives for the assembly of S-layer (Sap and EA1) and S-layer-associated proteins (BslA-U and AmiA) (5, 6, 35). Earlier work proposed that the genes for SCWP synthesis were located in the surface polysaccharide synthesis (*sps*) gene cluster (BAS5116 to BAS5127) (36). In agreement with this model, *gneZ* (BAS5117), which encodes a UDP-ManNAc epimerase, is essential for *B. anthracis* growth and SCWP synthesis (12). Nevertheless, *gneY*

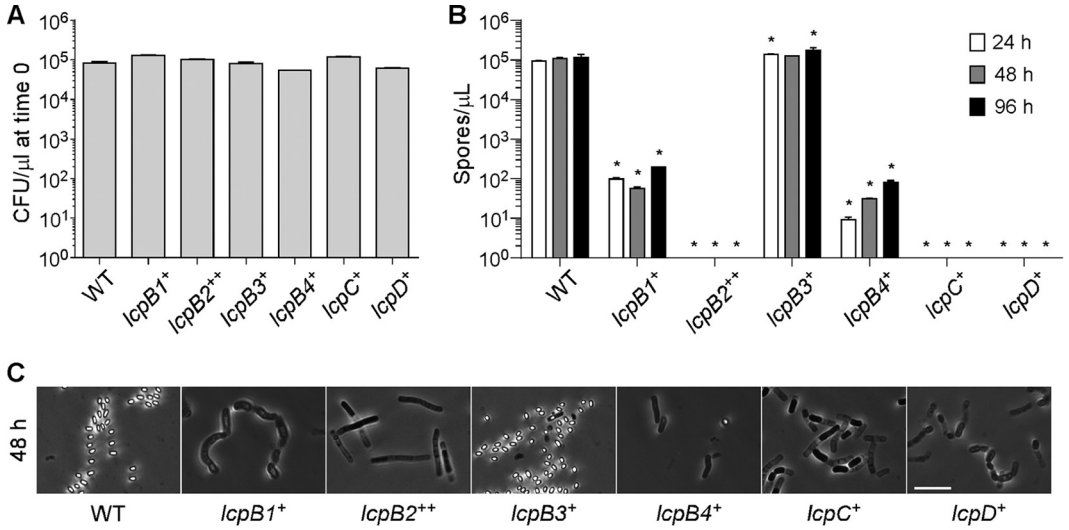

FIG 6 Sporulation efficiency of *lcp* variants. Bacilli from overnight cultures of *B. anthracis* Sterne (WT) and isogenic variants carrying a single *lcp* gene were washed, suspended in modG sporulation medium at an A_{600} of 1, and incubated at 30°C with shaking. (A) Culture aliquots were taken immediately following inoculation into modG medium, serially diluted, and plated to enumerate viable bacteria at time 0 (CFU). (B) Culture aliquots were collected at 24, 48, and 96 h following inoculation into modG medium, heat treated at 68°C for 30 min to kill vegetative bacilli, serially diluted, and plated to enumerate spores. (C) Culture aliquots from the 48-h time point were also fixed and visualized by phase-contrast microscopy. Representative images are shown. The scale bar represents 10 μm.

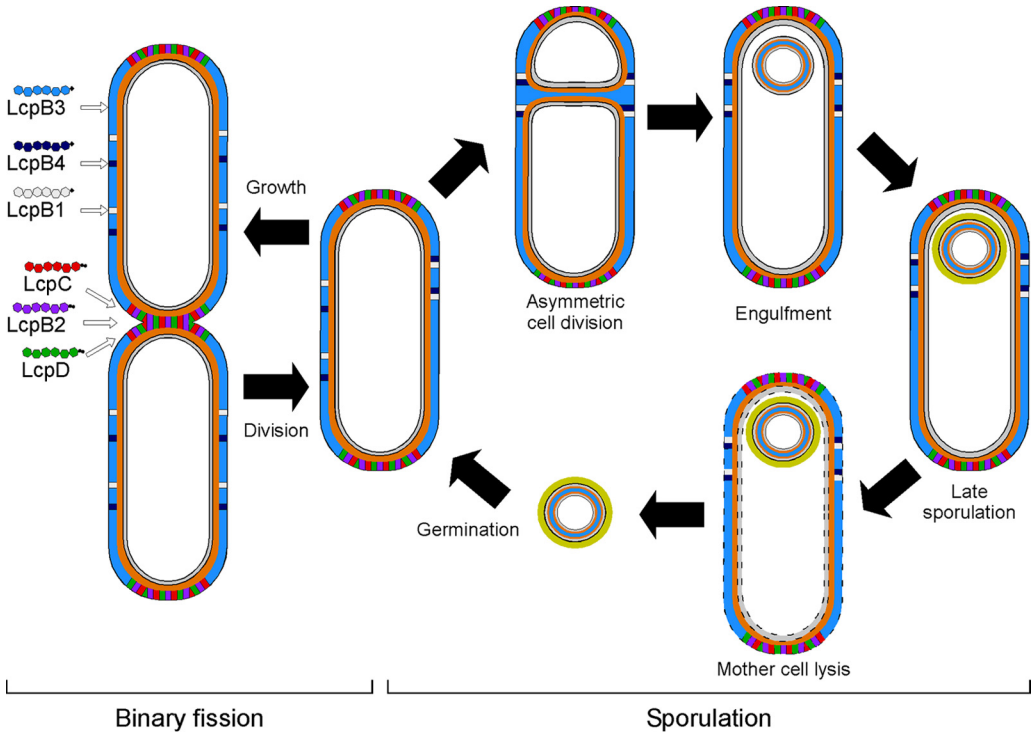

FIG 7 A model of possible functions of LytR-CpsA-Psr (LCP) proteins in *B. anthracis*. LCP proteins function to attach secondary cell wall polysaccharide (SCWP) to the peptidoglycan of *B. anthracis* cells. LcpB3 is the housekeeping LCP and attaches the majority of the SCWP. LcpB2, LcpC, and LcpD attach specialized SCWP to the cell poles and septa to enable proper deposition of S-layer and S-layer-associated proteins. LcpB1 and LcpB4 attach specialized SCWP along the midcell to allow for proper asymmetrical division during sporulation.

(BAS5048), a homolog of *gneZ*, can substitute for loss of *gneZ* function to restore *B. anthracis* growth and SCWP synthesis. *gneY* is part of another gene cluster also involved in SCWP synthesis; it includes *lcpD* (BAS5047) and *tagO* (BAS5050). *lcpC* (BAS5115) is also part of the *sps* gene cluster, whereas *lcpB1* (BAS1830), *lcpB2* (BAS0572), *lcpB3* (BAS0746), and *lcpB4* (BAS3381) are not associated with chromosomal genes known to be required for SCWP synthesis or assembly.

Previous work generated mutations that abolished the expression of individual *lcp* genes in *B. anthracis*, examining mutants for growth, cell size, chain length, SCWP synthesis, and S-layer assembly phenotypes. The *lcpD* mutant displayed increased chain length, diminished assembly of SCWP, and an S-layer protein assembly defect (13). In contrast, the *lcpB3* mutant formed smaller cells with reduced chain length and defects in BSL deposition into S-layer structures (13). The remaining mutants (*lcpB1*, *lcpB2*, *lcpB4*, and *lcpC* genotypes) did not reveal phenotypic defects. Here we show that deletions of several different *lcp* genes from the chromosome can be tolerated by *B. anthracis*, albeit all attempts to generate a strain expressing only genome-contained *lcpB2* failed. This could be circumvented by cloning *lcpB2* on a plasmid under the control of the constitutive *hprK* promoter (37). These data suggest that, as observed for *gneY*, *lcpB2* may not be expressed under laboratory conditions. Furthermore, *lcp* genes, similar to *gneZ* and *tagO*, are essential for *B. anthracis* vegetative growth (6, 12, 38). With the exception of the *lcpB3*$^+$ variant, all *B. anthracis* strains expressing single *lcp* gene were impaired for growth and displayed defects in cell size, chain length, and spore formation. Of note, the *lcpB3*$^+$ variant still assembled S-layers from Sap and EA1. These data suggest that LcpB3 likely transfers murein linkage units and SCWP with or without a ketal-pyruvyl modification to peptidoglycan, maintaining the housekeeping functions of the *B. anthracis* cell cycle and supporting assembly of the S-layer but not of BSLs. The *lcpC*$^+$ and *lcpD*$^+$ variants displayed severe growth, cell size, chain length, and S-layer assembly defects. Nonetheless, *lcpC*$^+$ and *lcpD*$^+$ variants were able to deposit BSLs into the bacterial envelope. We propose that LcpC and LcpD assemble SCWP with (LcpC) and without (LcpD) murein linkage units and PatA1/PatB1- or PatA2/PatB2-mediated acetylation of SCWP in the *B. anthracis* envelope. Finally, *B. anthracis* expressing only *lcpB1* (*lcpB1*$^+$) or only *lcpB4* (*lcpB4*$^+$) displayed moderate defects in cell size or shape, chain length, and spore formation, yet these variants sustained vegetative growth. Because the *lcpB1*$^+$ and *lcpB4*$^+$ strains, unlike the *lcpB3*$^+$ strain, display defects in S-layer and BSL assembly, we speculate that the preferred substrate of LcpB1 and LcpB4 may be specialized SCWP (Fig. 7). For example, specialized SCWP could carry terminal repeats that bear chemical modifications distinct from the known pyruvyl and acetyl groups (Fig. 7). Finally, we cannot rule out the possibility that some LCPs transfer as of yet unknown polymers in the envelope of *B. anthracis*.

lcpB1$^+$, *lcpB2*$^{++}$, and *lcpB4*$^+$ variants display reduced viability compared to *lcpB3*$^+$ bacteria. In addition, *lcpB1*$^+$, *lcpB2*$^{++}$, and *lcpB4*$^+$ variants fail to regulate chain length during the life cycle, and while their overall capacity to bind proteins with SLH domains is not affected, the deposition of these proteins is altered in the envelope. Deposition of proteins appears to be favored along the cylinder of *lcpB1*$^+$ and *lcpB4*$^+$ cells. This preferential deposi-

tion suggests that assembly of pyruvylated and acetylated SCWP, the receptor of SLH proteins, occurs at distinct sites in an LcpB-dependent manner when bacteria undergo binary fission, i.e., during vegetative replication, as illustrated in the model of Fig. 7. The *lcpC*$^+$ and *lcpD*$^+$ variants replicate poorly and display a marked reduction in their ability to retain SLH proteins in the envelope. Interestingly, these variants cannot sporulate, a phenotype not previously observed for genes involved in S-layer or SCWP assembly (6, 27, 35, 38). The inability to form spores (i.e., to shift the division site to undergo asymmetric cell division) may correlate with the failure to maintain the typical rod-shape morphology of vegetative cells. This defect may be caused by the inherent defect of *lcpC*$^+$ and *lcpD*$^+$ variants to homogenously assemble SCWP in the envelope of vegetative bacilli. We propose that all LCPs carry out attachment of SCWP, with LcpB3 being the most effective enzyme, followed by LcpB1, LcpB4, LcpB2, LcpC, and LcpD. This in turn correlates with the ability to form spores. Thus, we favor a model whereby LcpB2, LcpC, and LcpD influence biochemical reactions that are linked to the division site, whereas LcpB1 and LcpB4 promote reactions along the cylinder of rod-shaped bacilli.

ACKNOWLEDGMENTS

We thank members of our laboratory for discussion and comments on the manuscript, Derek Elli and Yating Wang for sharing reagents, and So-Young Oh for experimental support.

M.L.Z. and J.M.L. are trainees of the Medical Scientist Training Program at the University of Chicago and are supported by National Institutes of Health (NIH) Training Grant GM07281. J.M.L. is a recipient of NIH Ruth L. Kirschstein National Research Service Award 1F30AI110036-01. This research was supported by grant AI069227 from the National Institute of Allergy and Infectious Diseases, Infectious Disease Branch (to O.S. and D.M.).

REFERENCES

1. **Turnbull PC.** 1991. Anthrax vaccines: past, present and future. Vaccine **9:**533–539. http://dx.doi.org/10.1016/0264-410X(91)90237-Z.
2. **Mock M, Fouet A.** 2001. Anthrax. Annu Rev Microbiol **55:**647–671. http://dx.doi.org/10.1146/annurev.micro.55.1.647.
3. **Anderson VJ, Kern JW, McCool JW, Schneewind O, Missiakas D.** 2011. The SLH-domain protein BslO is a determinant of Bacillus anthracis chain length. Mol Microbiol **81:**192–205. http://dx.doi.org/10.1111/j.1365-2958.2011.07688.x.
4. **Ruthel G, Ribot WJ, Bavari S, Hoover T.** 2004. Time-lapse confocal imaging of development of *Bacillus anthracis* in macrophages. J Infect Dis **189:**1313–1316. http://dx.doi.org/10.1086/382656.
5. **Mesnage S, Fontaine T, Mignot T, Delepierre M, Mock M, Fouet A.** 2000. Bacterial SLH domain proteins are non-covalently anchored to the cell surface via a conserved mechanism involving wall polysaccharide pyruvylation. EMBO J **19:**4473–4484. http://dx.doi.org/10.1093/emboj/19.17.4473.
6. **Kern J, Ryan C, Faull K, Schneewind O.** 2010. *Bacillus anthracis* surface-layer proteins assemble by binding to the secondary cell wall polysaccharide in a manner that requires *csaB* and *tagO*. J Mol Biol **401:**757–775. http://dx.doi.org/10.1016/j.jmb.2010.06.059.
7. **Kern J, Wilton R, Zhang R, Binkowski TA, Joachimiak A, Schneewind O.** 2011. Structure of surface layer homology (SLH) domains from Bacillus anthracis surface array protein. J Biol Chem **286:**26042–26049. http://dx.doi.org/10.1074/jbc.M111.248070.
8. **Kern VJ, Kern JW, Theriot JA, Schneewind O, Missiakas D.** 2012. Surface-layer (S-layer) proteins Sap and EA1 govern the binding of the S-layer-associated protein BslO at the cell septa of Bacillus anthracis. J Bacteriol **194:**3833–3840. http://dx.doi.org/10.1128/JB.00402-12.
9. **Choudhury B, Leoff C, Saile E, Wilkins P, Quinn CP, Kannenberg EL, Carlson RW.** 2006. The structure of the major cell wall polysaccharide of *Bacillus anthracis* is species specific. J Biol Chem **281:**27932–27941. http://dx.doi.org/10.1074/jbc.M605768200.
10. **Forsberg LS, Abshire TG, Friedlander A, Quinn CP, Kannenberg EL, Carlson RW.** 2012. Localization and structural analysis of a conserved pyruvylated epitope in *Bacillus anthracis* secondary cell wall polysaccharides and characterization of the galactose deficient wall polysaccharide from avirulent *B. anthracis* CDC 684. Glycobiology **22:**1103–1117. http://dx.doi.org/10.1093/glycob/cws080.
11. **Velloso LM, Bhaskaran SS, Schuch R, Fischetti VA, Stebbins CE.** 2008. A structural basis for the allosteric regulation of non-hydrolysing UDP-GlcNAc 2-epimerases. EMBO Rep **9:**199–205. http://dx.doi.org/10.1038/sj.embor.7401154.
12. **Wang YT, Missiakas D, Schneewind O.** 2014. GneZ, a UDP-GlcNAc 2-epimerase, is required for S-layer assembly and vegetative growth of Bacillus anthracis. J Bacteriol **196:**2969–2978. http://dx.doi.org/10.1128/JB.01829-14.
13. **Liszewski Zilla M, Chan YG, Lunderberg JM, Schneewind O, Missiakas D.** 2015. LytR-CpsA-Psr enzymes as determinants of Bacillus anthracis secondary cell wall polysaccharide assembly. J Bacteriol **197:**343–353. http://dx.doi.org/10.1128/JB.02364-14.
14. **Kawai Y, Marles-Wright J, Cleverley RM, Emmins R, Ishikawa S, Kuwano M, Heinz N, Bui NK, Hoyland CN, Ogasawara N, Lewis RJ, Vollmer W, Daniel RA, Errington J.** 2011. A widespread family of bacterial cell wall assembly proteins. EMBO J **30:**4931–4941. http://dx.doi.org/10.1038/emboj.2011.358.
15. **Eberhardt A, Hoyland CN, Vollmer D, Bisle S, Cleverley RM, Johnsborg O, Havarstein LS, Lewis RJ, Vollmer W.** 2012. Attachment of capsular polysaccharide to the cell wall in Streptococcus pneumoniae. Microb Drug Resist **18:**240–255. http://dx.doi.org/10.1089/mdr.2011.0232.
16. **Chan YG, Frankel MB, Dengler V, Schneewind O, Missiakas D.** 2013. Staphylococcus aureus mutants lacking the LytR-CpsA-Psr family of enzymes release cell wall teichoic acids into the extracellular medium. J Bacteriol **195:**4650–4659. http://dx.doi.org/10.1128/JB.00544-13.
17. **Chan YG, Kim HK, Schneewind O, Missiakas D.** 2014. The capsular polysaccharide of Staphylococcus aureus is attached to peptidoglycan by the LytR-CpsA-Psr (LCP) family of enzymes. J Biol Chem **289:**15680–15690. http://dx.doi.org/10.1074/jbc.M114.567669.
18. **Kojima N, Arakai Y, Ito E.** 1985. Structure of the linkage units between ribitol teichoic acids and peptidoglycan. J Bacteriol **161:**299–306.
19. **Yokoyama K, Miyashita T, Arakai Y, Ito E.** 1986. Structure and functions of linkage unit intermediates in the biosynthesis of ribitol teichoic acids in *Staphylococcus aureus* H and *Bacillus subtilis* W23. Eur J Biochem **161:**479–489. http://dx.doi.org/10.1111/j.1432-1033.1986.tb10469.x.
20. **Sterne M.** 1937. Avirulent anthrax vaccine. Onderstepoort J Vet Sci Anim Ind **21:**41–43.
21. **Fulford W, Model P.** 1984. Specificity of translational regulation by two DNA-binding proteins. J Mol Biol **173:**211–226. http://dx.doi.org/10.1016/0022-2836(84)90190-6.
22. **Kim HU, Goepfert JM.** 1974. A sporulation medium for *Bacillus anthracis*. J Appl Bacteriol **37:**265–267. http://dx.doi.org/10.1111/j.1365-2672.1974.tb00438.x.
23. **Tam C, Glass EM, Anderson DM, Missiakas D.** 2006. Transposon mutagenesis of *Bacillus anthracis* strain Sterne using *bursa aurealis*. Plasmid **56:**74–77. http://dx.doi.org/10.1016/j.plasmid.2006.01.002.
24. **Marraffini LA, Schneewind O.** 2006. Targeting proteins to the cell wall of sporulating *Bacillus anthracis*. Mol Microbiol **62:**1402–1417. http://dx.doi.org/10.1111/j.1365-2958.2006.05469.x.
25. **Gaspar AH, Marraffini LA, Glass EM, Debord KL, Ton-That H, Schneewind O.** 2005. Bacillus anthracis sortase A (SrtA) anchors LPXTG motif-containing surface proteins to the cell wall envelope. J Bacteriol **187:**4646–4655. http://dx.doi.org/10.1128/JB.187.13.4646-4655.2005.
26. **Green BD, Battisti L, Koehler TM, Thorne CB, Ivins BE.** 1985. Demonstration of a capsule plasmid in *Bacillus anthracis*. Infect Immun **49:**291–297.
27. **Nguyen-Mau SM, Oh SY, Kern VJ, Missiakas DM, Schneewind O.** 2012. Secretion genes as determinants of Bacillus anthracis chain length. J Bacteriol **194:**3841–3850. http://dx.doi.org/10.1128/JB.00384-12.
28. **Neuhaus FC, Baddiley J.** 2003. A continuum of anionic charge: structures and functions of D-alanyl-teichoic acids in gram-positive bacteria. Microbiol Mol Biol Rev **67:**686–723. http://dx.doi.org/10.1128/MMBR.67.4.686-723.2003.
29. **Lazarevic V, Pooley HM, Mauel C, Karamata D.** 2002. Teichoic and teichuronic acids from Gram-positive bacteria, p 465–492. *In* Vandamme

EJ, De Baets S, Steinbuchel A (ed), Polysaccharides from prokaryotes, vol 5. Wiley-VCH Verlag, Weinheim, Germany.
30. **Soldo B, Lazarevic V, Karamata D.** 2002. *tagO* is involved in the synthesis of all anionic cell-wall polymers in *Bacillus subtilis* 168. Microbiology **148:** 2079–2087. http://dx.doi.org/10.1099/00221287-148-7-2079.
31. **Dengler V, Meier PS, Heusser R, Kupferschmied P, Fazekas J, Friebe S, Staufer SB, Majcherczyk PA, Moreillon P, Berger-Bachi B, McCallum N.** 2012. Deletion of hypothetical wall teichoic acid ligases in Staphylococcus aureus activates the cell wall stress response. FEMS Microbiol Lett **333:**109–120. http://dx.doi.org/10.1111/j.1574-6968.2012.02603.x.
32. **Brown S, Santa Maria JP, Jr, Walker S.** 2013. Wall teichoic acids of Gram-positive bacteria. Annu Rev Microbiol **67:**313–336. http://dx.doi.org/10.1146/annurev-micro-092412-155620.
33. **Xia G, Kohler T, Peschel A.** 2010. The wall teichoic acid and lipoteichoic acid polymers of Staphylococcus aureus. Int J Med Microbiol **300:**148–154. http://dx.doi.org/10.1016/j.ijmm.2009.10.001.
34. **Molnár J, Prágai B.** 1971. Attempts to detect the presence of teichoic acid in *Bacillus anthracis*. Acta Microbiol Acad Sci Hung **18:**105–108.
35. **Lunderberg JM, Nguyen-Mau SM, Richter GS, Wang YT, Dworkin J, Missiakas DM, Schneewind O.** 2013. Bacillus anthracis acetyltransferases PatA1 and PatA2 modify the secondary cell wall polysaccharide and affect the assembly of S-layer proteins. J Bacteriol **195:**977–989. http://dx.doi.org/10.1128/JB.01274-12.
36. **Schuch R, Pelzek AJ, Raz A, Euler CW, Ryan PA, Winer BY, Farnsworth A, Bhaskaran SS, Stebbins CE, Xu Y, Clifford A, Bearss DJ, Vankayalapati H, Goldberg AR, Fischetti VA.** 2013. Use of a bacteriophage lysin to identify a novel target for antimicrobial development. PLoS One **8:**e60754. http://dx.doi.org/10.1371/journal.pone.0060754.
37. **Bubeck Wardenburg J, Williams WA, Missiakas D.** 2006. Host defenses against Staphylococcus aureus infection require recognition of bacterial lipoproteins. Proc Natl Acad Sci U S A **103:**13831–13836. http://dx.doi.org/10.1073/pnas.0603072103.
38. **Lunderberg JM, Liszewski Zilla M, Missiakas D, Schneewind O.** 31 August 2015. Bacillus anthracis tagO is required for vegetative growth and secondary cell wall polysaccharide synthesis. J Bacteriol http://dx.doi.org/10.1128/JB.00494-15.